

The crystal structure of ionic conductor $\text{La}_x\text{Ce}_{1-x}\text{O}_{2-x/2}$

Jong Sung Bae^{a,*}, Woong Kil Choo^a, Chang Hee Lee^b

^aDepartment of Materials Science and Engineering, Korea Advanced Institute of Science and Technology, 373-1 Gusong-Dong, Yusong-Gu, Daejeon, South Korea

^bNeutron Beam Application Project, HANARO Center, Korea Atomic Energy Research Institute, Daejeon 305-600, South Korea

Abstract

The crystal structure of La^{3+} substituted CeO_2 solid solution ($\text{La}_x\text{Ce}_{1-x}\text{O}_{2-x/2}$) has been investigated by X-ray and neutron powder diffractions. The fluorite structure of CeO_2 is still maintained up to $x=0.4$ composition although La^{3+} is the largest trivalent rare earth ion. For $x \geq 0.5$ the crystal structure changes to the pyrochlore cation ordering and the remnant La_2O_3 is unreacted. This structure can, however, be stabilized by Ti^{4+} addition or thermal treatment.

© 2003 Elsevier Ltd. All rights reserved.

Keywords: Crystal structure; Ionic conductor; Solid solution; X-ray; Neutron

1. Introduction

CeO_2 solid solutions with rare earth oxides has been much investigated as electrolyte in solid oxide fuel cells (SOFC) due to its higher oxygen conductivity than that of ZrO_2 solid solution.^{1–9} It has been reported that the ionic conductivity of solid solution strongly depends on the ionic radius of the substituent.^{10,11} Inaba and Tagawa⁵ explained that the maximum conductivity is obtained when the ionic radius of the substituent is close to that of the host ion due to the low strength of the association energy in the crystal structure. So, information about the crystal structure is important because it clarifies the correlation between atoms related with ionic radius and ionic transportation.

The structural study of La^{3+} substituted CeO_2 , $\text{La}_x\text{Ce}_{1-x}\text{O}_{2-x/2}$ solid solution, has only sketchily been investigated.¹² La^{3+} is of the largest size among the trivalent rare earth ions such that the size difference between Ce^{4+} and La^{3+} is large. The crystal structure change of CeO_2 by La substitution and the stabilization of fluorite structure deserve to be scrutinized.

2. Experimental

$\text{La}_x\text{Ce}_{1-x}\text{O}_{2-x/2}$ was synthesized by solid state reaction of the mixed La_2O_3 , CeO_2 powders at 1400 °C for 7

h. Ti^{4+} is added by sintering TiO_2 together with the rest of the powders. X-ray powder diffraction patterns were collected at room temperature on a Rigaku Rotaflex diffractometer using $\text{CuK}\alpha$ radiation equipped with a graphite monochromator [$\lambda = 1.5418 \text{ \AA}$, $2\theta = 20^\circ \sim 130^\circ$]. X-ray output power was 40 kV, 120 mA. Long time step scanning was performed to enlarge the intensity of the superlattice reflections which are usually of very low intensity. The neutron powder diffraction pattern was collected at various temperatures on a high-resolution powder diffractometer (HRPD) [$\lambda = 1.8430 \text{ \AA}$, $2\theta = 20^\circ \sim 130^\circ$] at the Hanaro reactor, Korea Atomic Energy Research Institute. Test powders were compacted in a vanadium cylinder and were cooled and heated in vacuum. Neutron beams from the reactor were monochromated by a Ge(331) single crystal.

3. Results and discussion

Fig. 1 is the X-ray diffraction profile of $\text{La}_x\text{Ce}_{1-x}\text{O}_{2-x/2}$ at room temperature. A rather simple pattern implying a high symmetry is observed. Only the fundamental reflections, no extra diffraction lines are shown. It shows that a single phase can be obtained by calcining the mixture of constituent oxides from $x=0$ –0.4. It means that the CeO_2 structure can fully accommodate larger La^{3+} up to 40%. Furthermore, the fluorite structure of CeO_2 is still maintained in spite of La substitution. CeO_2 is well known to possess the fluorite structure in which cations form a face centered cubic array and

* Corresponding author. Tel.: +82-42-869-4278; fax: +82-42-869-33100.

oxygen atoms are located in the tetrahedral sites. So the fundamental XRD peaks can be indexed with face-centered symmetry.

However, a second phase precipitates in La^{3+} 50% substituted, $\text{La}_2\text{Ce}_2\text{O}_7$, as presented in the XRD pattern of Fig. 2. Low intensity lines which represent superstructure originated from pyrochlore cation ordering is observed. The second phase lines are marked by filled circles and the superlattice lines are marked by open squares. Unidentifiable lines are marked by 'x'. This result is replicated in the neutron diffraction pattern of $\text{La}_2\text{Ce}_2\text{O}_7$ as represented in Fig. 3. 'F' represents fundamental reflection of the fluorite structure in the figure.

Pyrochlore oxide compound, $\text{A}_2\text{B}_2\text{O}_7$, is of a superstructure based on a fluorite type arrangement of cations and anions. Cations are located at the sites surrounded by 8-fold coordination polyhedra of oxygens for A and by 6-fold coordination polyhedra for B respectively. It is conjectured that the driving force for cation ordering is the size difference of cations.

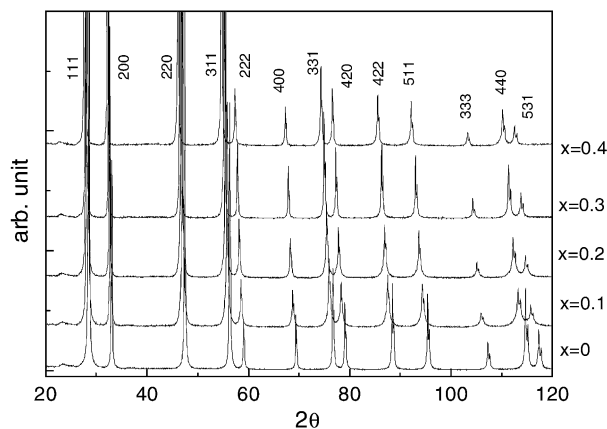


Fig. 1. X-ray diffraction profile of $\text{La}_x\text{Ce}_{1-x}\text{O}_{2-x/2}$ with composition at room temperature. Only the fundamental face center cubic lines are identified.

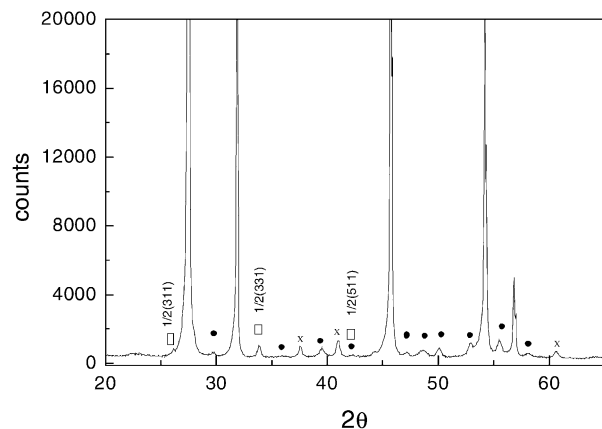


Fig. 2. XRD pattern of La^{3+} 50% substituted $\text{La}_2\text{Ce}_2\text{O}_7$ at room temperature. Low intensity ordering lines marked by squares, the second phase lines marked by filled circles and unidentifiable lines marked by 'x's are present.

Pyrochlores can be formed when the ionic radius ratio, RR , is in the range 1.46–1.80 at the ambient atmospheric pressure. From the ionic radii data taken from Muller and Roy,¹⁴ the ionic size of La^{3+} is 1.32 Å, that of Ce^{4+} is 0.94 Å. $\text{RR}(r_{\text{La}}/r_{\text{Ce}})$ is 1.40. Since the size difference between the two rare earth ions is not large enough, the pyrochlore structure may not globally be formed. However, it is conjectured that La^{3+} and Ce^{4+} cations may move to the ordering positions in some local areas of the 1:1 high ordering. For $x \geq 0.5$ mixture, La_2O_3 compound lines ascribed to the C-rare earth structure become larger with the increase of La composition while the superlattice line diminish. Fig. 4, the XRD pattern of La 60% and La 70% substituted CeO_2 shows such tendency.

The precipitation of constituent oxide compound and cation ordering in $\text{La}_x\text{Ce}_{1-x}\text{O}_{2-x/2}$ for $x \geq 0.5$ can be suppressed by thermal treatment or by adding small size tetravalent Ti^{4+} ions. Fig. 5 represents the high intensity XRD pattern of $\text{La}_2(\text{Ce}_{0.8}\text{Ti}_{0.2})_2\text{O}_7$ solid solution in which 20% Ti^{4+} ions substituted Ce^{4+} ion. Fig. 6 represents the high intensity XRD pattern of $\text{La}_2\text{Ce}_2\text{O}_7$ annealed at 1600 °C for 10 h under ambient

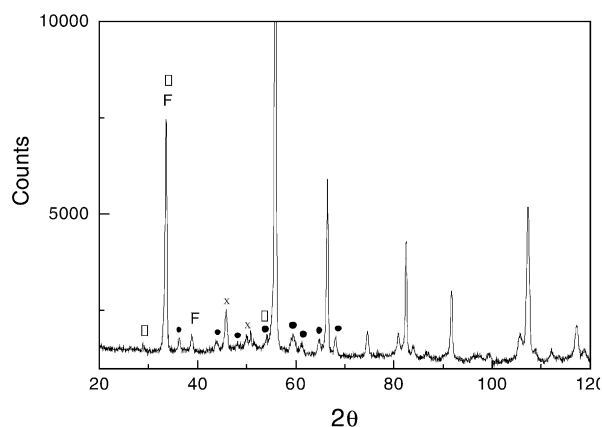


Fig. 3. Neutron diffraction pattern of $\text{La}_2\text{Ce}_2\text{O}_7$ at room temperature.

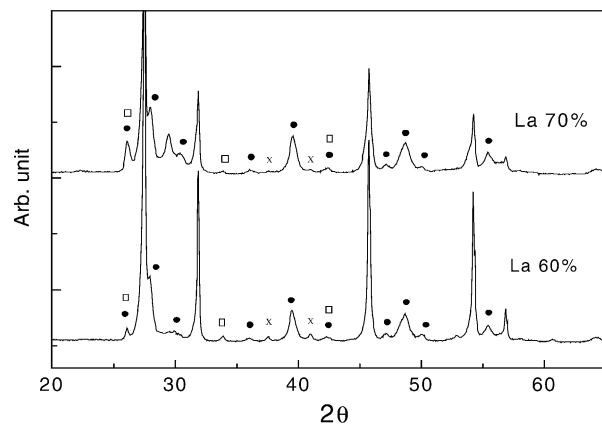


Fig. 4. XRD pattern of sintered La 60% and La 70% substituted CeO_2 .

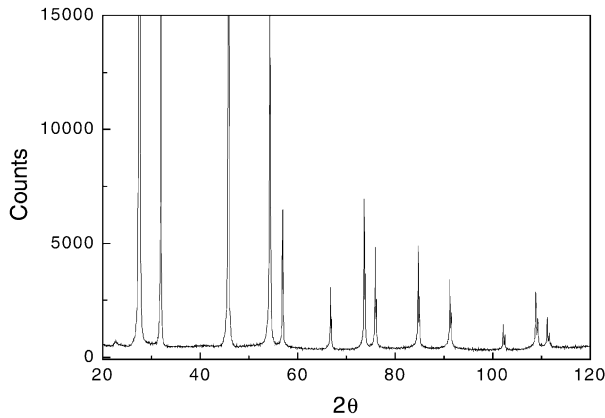


Fig. 5. XRD pattern of $\text{La}_2(\text{Ce}_{0.8}\text{Ti}_{0.2})_2\text{O}_7$ compound in which Ce^{4+} ions are substituted by Ti^{4+} about 20%. We can recognize this compound structure is almost identical.

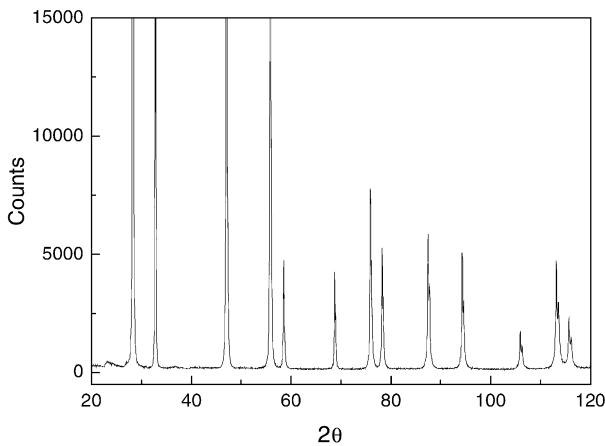


Fig. 6. XRD pattern of $\text{La}_2\text{Ce}_2\text{O}_7$ solid solution annealed at 1600 °C for 10 h under ambient atmosphere.

atmosphere. This figure shows that the XRD pattern of annealed $\text{La}_2\text{Ce}_2\text{O}_7$ is quite similar to that of CeO_2 . From the above two simple experiments, precipitation and cation ordering may be suppressed.

The fcc lattice parameter of $\text{La}_x\text{Ce}_{1-x}\text{O}_{2-x/2}$ (for $0 \leq x \leq 0.5$) has been measured from the XRD pattern. Compared with the theoretical value based on the oxygen vacancy model, large deviation is observed at the high x region as shown in Fig. 7. The theoretical curve is calculated by the following equation based on the constituent ionic radii.¹⁵

$$a = \frac{4}{\sqrt{3}} [r_M - r_{ce} - 0.25r_o + 0.25r_{V_o}] \quad (1)$$

$$x + \frac{4}{\sqrt{3}} [r_{ce} + r_o]$$

where the subscripts mean $M = \text{La}^{3+}$, $\text{Ce} = \text{Ce}^{4+}$, $\text{O} = \text{O}^{2-}$ and V_o means oxygen vacancy. This deviation means the unit cell volume of the fluorite structure may contract by coalescence of vacancies. In the high La^{3+}

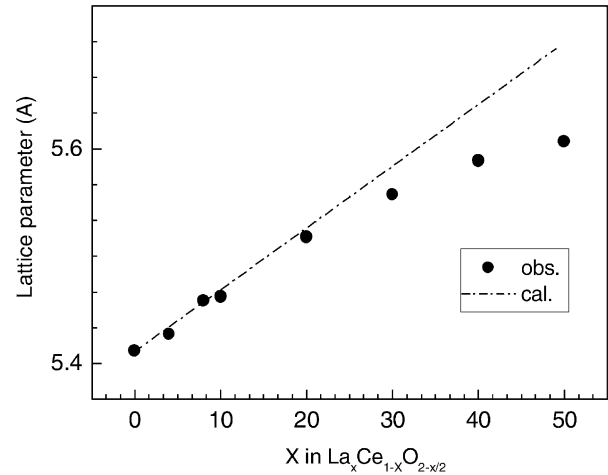


Fig. 7. The lattice parameters of $\text{La}_x\text{Ce}_{1-x}\text{O}_{2-x/2}$ ($x = 0$ to 0.5) measured from the XRD pattern.

substitution region, this deviation gets even larger most likely because more vacancies are generated and coalesce.

4. Conclusion

In the La^{3+} substituted CeO_2 solid solution the fluorite structure is very stable up to La 40% substitution in spite of much larger La ion size. However, some pyrochlore cation ordering between La^{3+} and Ce^{4+} occurs in the 50% La substitution. At the same time, $\text{La}_x\text{Ce}_{1-x}\text{O}_{2-x/2}$ is decomposed into La_2O_3 and CeO_2 gradually beyond 50% substitution. But, the intrinsic fcc CeO_2 structure can be stabilized by Ti^{4+} addition or thermal treatment at 1600 °C. This means that the lattice distortion caused by La^{3+} substitution of much larger ionic size is obstruction to forming a complete solid solution for $x \geq 0.5$ and provides for the driving force for cation ordering.

Acknowledgements

This research was achieved by the support of research reactor(HANARO) utilization plan 2001' in Korea. The Authors deeply appreciate the support.

References

1. Tuller, H. L. and Nowick, A. S., Doped ceria as a solid oxide electrolyte. *J. Electrochem. Soc.*, 1975, **122**, 255–259.
2. Yahiro, H., Ohuchi, T., Eguchi, K. and Arai, H., Electrical properties and microstructure in the system ceria-alkaline earth oxide. *J. Mater. Sci.*, 1988, **23**, 1036–1041.
3. Blumenthal, R. N., Brugner, F. S. and Garnier, J. E., The electrical conductivity of CaO-doped nonstoichiometric cerium dioxide from 700 to 1500 °C. *J. Electrochem. Soc.*, 1973, **120**, 1230–1237.

4. Blumenthal, R. N. and Garnier, J. E., The electrical conductivity and thermodynamic behavior of Sr-O-doped nonstoichiometric ceramic dioxide. *J. Solid State Chem.*, 1976, **16**, 21–34.
5. Inaba, H. and Tagawa, H., Ceria-based solid electrolytes-Review. *Solid State Ionics*, 1996, **83**, 1–16.
6. Kudo, T. and Obayashi, H., Mixed electrical conduction in the fluorite-type $\text{Ce}_{1-x}\text{Gd}_x\text{O}_{2-x/2}$. *Electrochem. Soc.*, 1976, **123**, 415–419.
7. Christie, G. M. and Berkel, F. P. F., Microstructure—Ionic conductivity relationships in ceria-gadolinia electrolytes. *Solid State Ionics*, 1996, **83**, 17–27.
8. Yahiro, H., Eguchi, Y., Eguchi, K. and Arai, H., Oxygen ion conductivity of the ceria-samarium oxide system with fluorite structure. *J. Appl. Electrochem*, 1988, **18**, 527.
9. Mori, T., Yamamura, H. and Saito, S., Preparation of an alkali-element-doped $\text{CeO}_2\text{-Sm}_2\text{O}_3$ system with fluorite structure. *J. Am. Ceram. Soc.*, 1996, **79**, 3309–3312.
10. Gerhardt-Anderson, R. and Nowick, A. S., Ionic conductivity of CeO_2 with trivalent dopants of different ionic radii. *Solid State Ionics*, 1981, **5**, 547.
11. Butler, V., Catlow, C. R. A., Fender, B. E. F. and Harding, J. H., Dopant ion radius and ionic conductivity in cerium dioxide. *Solid State Ionics*, 1983, **8**, 109.
12. Morris, B. C., Flavell, W. R., Mackrodt, W. C. and Morris, M. A., lattice parameter changes in the mixed oxide system $\text{Ce}_{1-x}\text{La}_x\text{O}_{2-x/2}$ —a combined experimental and theoretical study. *J. Mater. Chem.*, 1993, **3**(10), 1007.
13. Subramanian, M. A., Aravamudan, G. and Rao, G. V. S., Oxide pyrochlores—a review. *Prog. Solid State. Chem.*, 1983, **15**, 55.
14. Muller, O. and Roy, R., *The Major Tendency Structural Families*. Springer-Valley, Berlin, 1974.
15. Hong, S. J. and Virkar, A. V., Lattice parameters and densities of rare-earth oxide doped ceria electrolytes. *J. Am. Ceram. Soc.*, 1995, **78**, 433.